JScholar
Fostering Scholarly Communication

Photocatalytic Degradation of Organic Dyes Using Nanocrystalline Mg-Co Ferrite

Jadhav SD*and Patil RS

Department of Chemistry, Yashwantrao Chavan College of science, Karad Shivaji University, India

***Corresponding author:** Jadhav SD, Department of Chemistry, Yashwantrao Chavan College of science, Karad Shivaji University, India, Tel: 91 9881847898; Email: sdjchemsuk@gmail.com; sdj_chem2007@rediffmail.com

Abstract

The semiconducting Mg-Co ferrite nanoparticles prepared via controlled co-precipitation method. The X-ray diffraction and Transmission Electron Microscopy (SAED patterns) techniques were employed to study phase, composition and the average particle size of the resulting material. The photocatalytic degradation of methyl orange and Congo red dye were performed under illumination of visible light (Philips 250Watt) as source of photons. The behavior of this reaction was pseudo first order and the maximum photodecolorization efficiency was 85.16% for Methyl orange and 95.40 for Congo red in 60 min. at 30°C

Keywords: X-ray Diffraction, SEM, Transmission electron microscopy (TEM), Photo catalysis

Introduction

Water contamination is mainly caused due to toxic effluents drain by number of chemical, agricultural and textile industries. It has been reported that about 25% dye stuffs discharged directly into the environment by textile factory. Generally, waste water generated by textile industry contains considerable amount of non-fixed dyes, especially azo dyes and a huge amount of inorganic salts. Also contains several non-biodegradable substrates that can be harmful to the environment. Their toxicity, stability to natural decomposition and persistence in the environment has been the cause of much concern to the society and regulation authorities all around the world [1-3]. Environmental problems associated with toxic organic pollutants in water and air is current issues to be solved for the development of a healthy environment.

Photocatalytic oxidation is one of the emerging technologies for the decomposition of organic dyes such as Reactive black 5, Acid orange, Aniline yellow, Orange B, Methyl yellow, Methyl red, Methyelene blue, Congo red & Methyl orange etc. Azo dyes represent about one-half of the dyes used in the textile industry. Among azo dyes, Methyl Orange (MO) is highly water soluble, even at very low concentrations, which hinder the penetration of light and therefore cause adverse effects on photosynthesis. Congo Red (CR) was the first synthetic dye that could dye cotton directly [4]. It is contained in wastewater effluents from the textile, printing and dyeing, paper, rubber and plastics industries. CR is used in medicine as a biological stain and as an indicator since it turns from red-brown in a basic medium to blue in an acidic one. These are the different ways organic pollutants (dyes) continuously get added into water sources. Incomplete decomposition of organic pollutants may lead to formation of more toxic byproducts than the parent pollutants. Therefore, in order to overcome such problem looking for metal oxide photocatalyst with strong photodegradation capacity is inventible.

For instance, Jang et al. [5] and Jung et al. [6] respectively demonstrated that $ZnFe_2O_4$ and $CaFe_2O_4$ systems are useful for solar photocatalytic degradation of pollutants. Similarly, in case of homo [7] or hetero [8] composite ferrite systems, $CaFe_2O_4:MgFe_2O_4$ and $ZnFe_2O_4:SrTiO_3$ have been shown to be efficient and useful for photocatalytic water splitting. It has been reported that Ching Cheng *et al* [9] investigated the effects of cation distribution in $CdFe_2O_4$, M. Yokoyama *et al* [10] studied the magnetic properties of cadmium ferrite prepared by coprecipitation, Ashok Gadkaria *et al* [11] reported on structural and magnetic properties of $CdFe_2O_4$ ferrites, silva o *et al.* [12] reported the magnetic resonance investigation of cadmium ferrite. Cai et al. developed $ZnFe_2O_4$ via a reduction-oxidation method which showed degradation of Orange II dye [13], Sharma et al. MFe_2O_4 (M=Co, Ni, Cu, Zn) prepared by sol-gel method used for degradation of Methyl blue dye [14], Dhiman et al. reported $NiFe_2O_4$ visible light assisted photocatalytic degradation of Safranine - O dye and remazol brillent yellow at pH 2.5 [15] S. D. Jadhav et al. used $ZnFe_2O_4$ for degradation of Methyl orange dye [16] Hankare et al. studied $CoFe_2O_4$ prepared by sol-gel method for degradation of methylene blue[17]. The ferrites offer an advantage of displaying the desirable optical absorption for the low energy photons (hv ~2eV), and of exhibiting the well suited electronic structure desirable for photocatalytic applications [18]. This contrasts with the very popular anatase TiO_2 reference material, whose band gap of 3.2 eV allows only the absorption of UV light, corresponding to wavelengths lower than 388 nm [19]. On the other hand, especially photocatalyst are non-magnetic such as semiconductors (TiO_2, ZnO and ZnS) their separation and recovery after treatment is difficult [20]. Consequently, the problem of insufficient recovery not only leads to loss of photocatalyst but also the residual photocatalyst become additional environmental problem. Therefore, the effective and complete decolorization of organic pollutants containing wastewater is an important and challenging task. To make full use of solar energy, many attempts have been made to prepare the narrow band gap ferrite semiconducting material that utilizes the much larger visible region. Some of the recent reports can be important indicators with respect to the potential of visible light photocatalytic application of the spinel ferrites. Spinel ferrites which are mixed oxides of iron and a single or numerous metals are one such example of visible-light absorbing inorganic semiconductors studied for their photo catalytic activity due to their attractive photochemical properties such narrow optical, band gap (~2.0eV), good photochemical stability [21], recovery of photocatalyst and their relative stability in acidic and basic conditions. magnetic and optoelectronic properties [22]. They have strong photodegradation capacities; also improve the degradation rate of pollutants, ease the from the reaction mixture after being used and enhance Consequently they are very useful for the complete removal of organic pollutants [23-25].

To the best of our knowledge, as per the literature there are few reports has been cited in the literature on the photocatalytic properties of divalent metal ion doped cobalt ferrite nanoparticles under solar light irradiation. Accordingly, in this paper we reported photocatalytic degradation of azo dye using magnesium doped cobalt ferrite nanoparticals.

Experimental

Materials

Methyl orange and Congo red dye was supplied by Sigma Aldrich which a physico-chemical characteristic that is has illustrated in (Figure 1) and (Table 1)
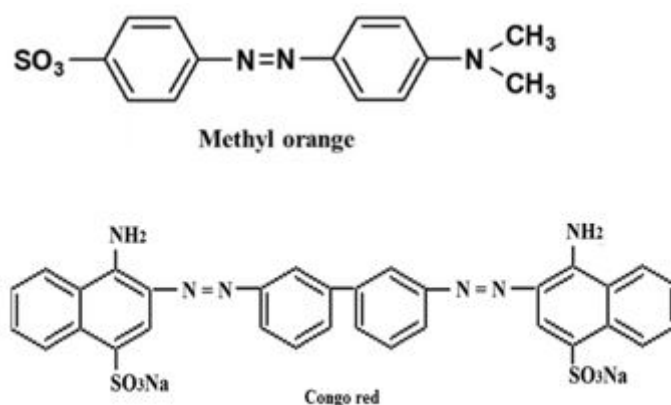
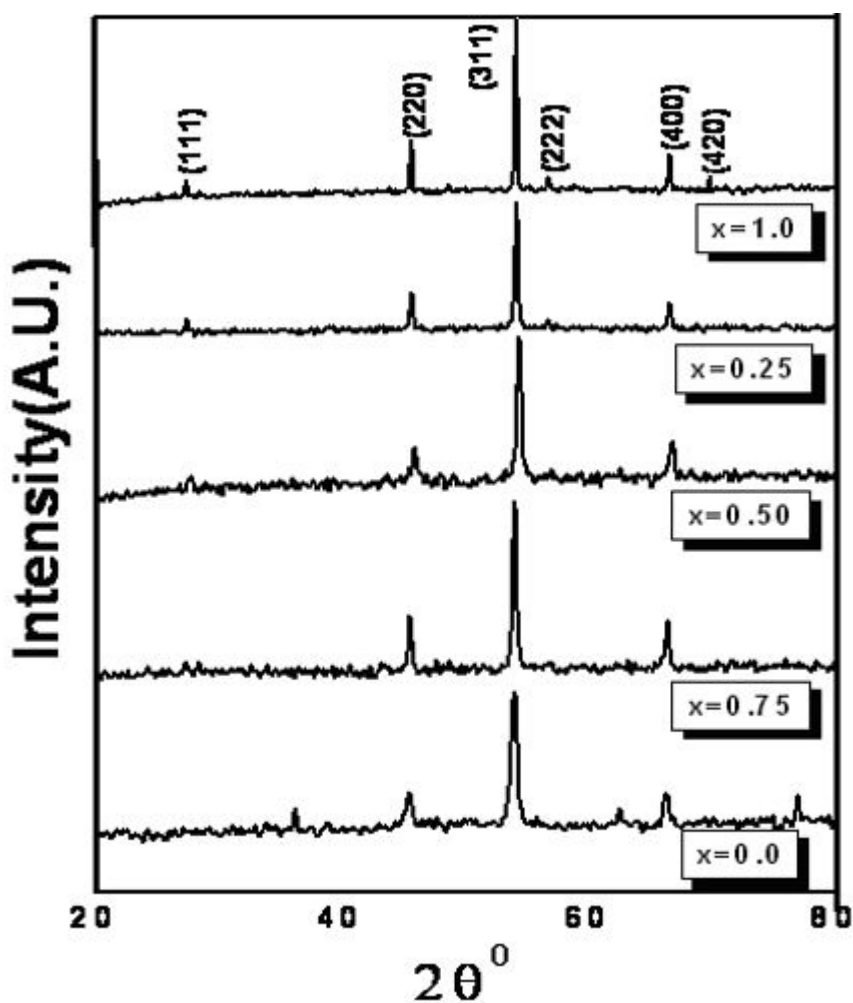The structural formula of Methyl orange and Congo red dye dye

Figure 1: XRD Patterns for the $Mg_{1-x}Co_xFe_2O_4$ system sintered at 600^0C ($0 \leq x \leq 1$)

Table 1. Physico-chemical characteristics of the Methyl orange and Congo red dye

Parameters	Methyl orange	Congo red
Synonym	54	
7-58-0 Orange III	Direct red 28	
Molecular Weight	327.33g/mol	696.665g/mol
Molecular formula	$C_{14}H_{14}N_3O_3SNa$	$C_{32}H_{22}N_6Na_2O_6S_2$
Type	Acid dye	Acid-Basic Indicator
λmax	460-470 nm	497-498 nm
Solubility in water	*Sol*uble	Soluble

Method

The Mg-Co ferrite has been synthesized by using controlled co-precipitation technique [26]. The series of the photo-reaction experiments were conducted by mixing 100 mL from aqueous solution of Methyl orange and Congo red with a suitable amount of $Mg_{0.5}Co_{0.5}Fe_2O_4$ nanopowder as suspension solution. In fact, the equilibrium time for this reaction was closely performed at 30 min as adsorption process. Visible light bulbs containing tungsten filament (Philips 250 W) were applied as a source of photons; it was connected at the top of the reactor chamber [27]. Light intensity value equal to 1.48×10^{-7} Ens. s^{-1}, which calculated by chemical actinometrical solution [28]. With regular intervals, certain amount of samples were collected and double separated by centrifuge to remove all photocatalyst from dye solutions. The filtered dye solutions were analysed to determine the residue concentration of dye by recording the absorbance at 464 nm and 500nm using UV visible spectrophotometer.

By depended on Langmuir-Henshelwood mechanism, the rate constant was determined [29], and the photodecolorization efficiency (PDE%) was calculated by the following equation [30].

$$In\ (Co/Ct) = Kapp.\ x\ t \dots\dots\dots\dots(1)$$

$$PDE\% = \frac{Co-Ct}{Co}\ x\ 100 \dots\dots\dots\dots(2)$$

Here: Co is an initial concentration of methyl Orange and Congo red dyes at no irradiation time (min). Ct is a concentration of the same dye at t time of irradiation (min).
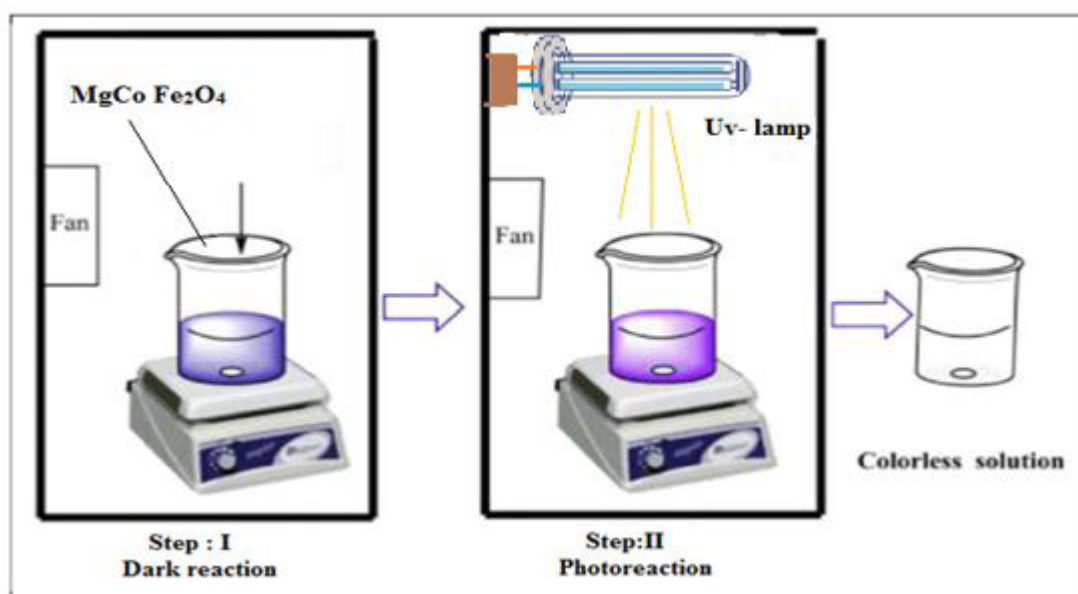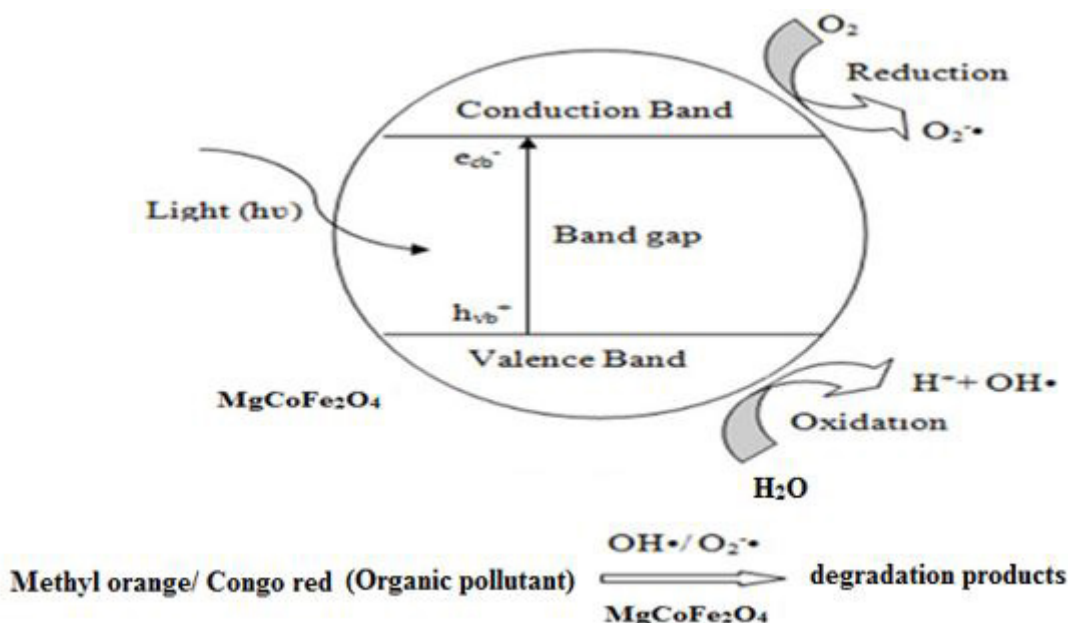
Results and Discussion

Characterization

The X-ray diffraction patterns of the system $Mg_{1-x}Co_xFe_2O_4$ (x = 0.0 to 1.0) sintered at 600°C as shown in (Figure 1). All the indexed diffraction peaks corresponding to the (111), (220), (311), (400), (422) and (511) planes of polycrystalline spinel ferrite [31]. The X-ray lines found to be sharp which makes detection of phases easy. All spinel composition shows (311) peak is the more intense one. The d_{hkl} and 2θ values were compared with the values reported in the literature (cubic, $MgFe_2O_4$, JCPDS file No. 73-1720) and (cubic, $CoFe_2O_4$, JCPDS file No. 22-1086).

The SEM micrograph shows the formation of polycrystalline grains. From this image, it can be seen that most of the grains are of size about ~30nm (Figure 2a). Transmission electron micrographs of $Mg_{0.5}Co_{0.5}Fe_2O_4$ system depict in (Figure 2 b & c). The corresponding selected area electron diffractograms (SAEDs) are given as an inset. It is evident from these micrographs that all the synthesized samples have spherical particles ranging from 30 to 40 nm. The superimposition of the bright spot with Debye ring pattern indicates polycrystalline nature of the sample. Both the figures confirm that most of the particles are of size about 30 nm.


(a)
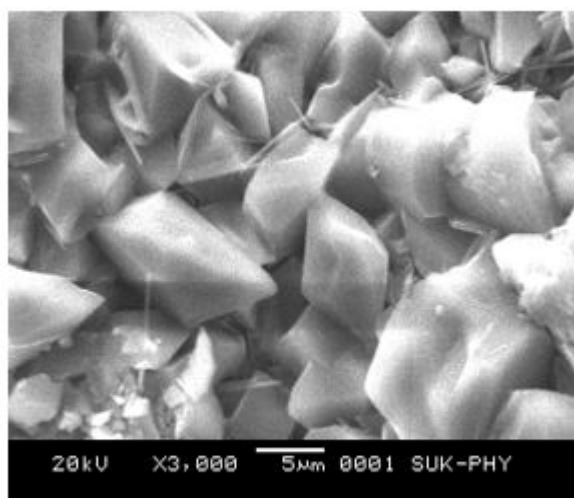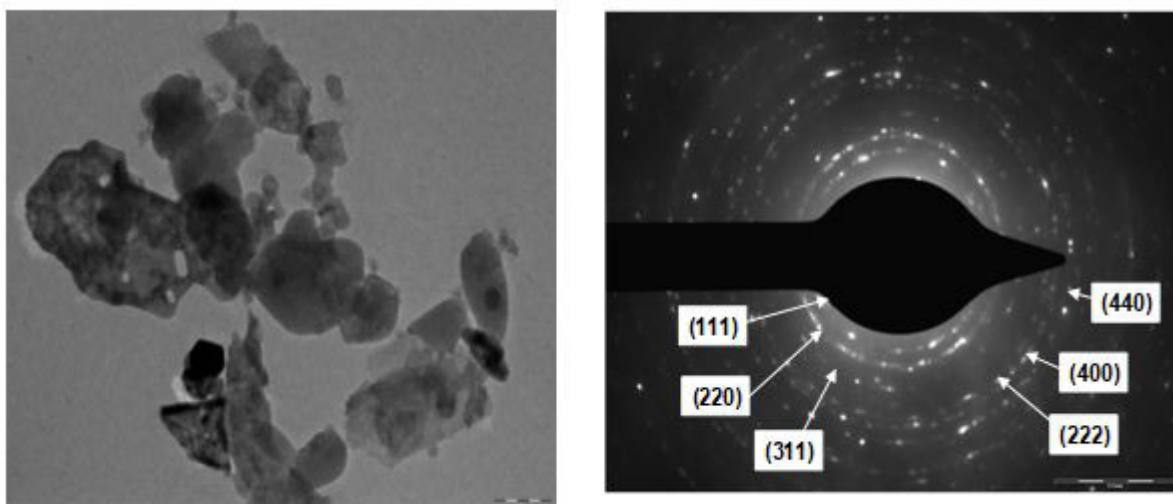
Fiigure 2: (a) Scanning electron micrograph **(b)** Transmission electron micrograph **(c)** SAED pattern for $Mg_{0.5}Co_{0.5}Fe_2O_4$ sintered at 600°C

Effect Of Irradiation Time on Photodegradation Of Methyl Orange And Congo Red Dyes

To test the photocatalytic (PC) properties of $Mg_{0.5}Co_{0.5}Fe_2O_4$, the kinetics of the degradation of a pollutant model, methyl orange (MO) and Congo red (CR), were followed in water, under UV light (250W) illumination. The intensity of the characteristic absorption bands of MO & CR centered at about 460-470 nm and 498- 502nm respectively [32], was measured every 30min. The degradation of MO solution was selected as reference and characterstic absorption of MO solution at about 464 nm was selected for monitoring adsorption and photocata-lytic degradation process. A significant decrease in transmittance at about 460nm can be assigned to absorption of light caused by the excitation of electrons from valence ban to the conduction band of MO solution (Figure 3). For CR there was complete absorption of light by CR solution, the absorption peak at 500nm disappears and no peak shift can be detected after degradation treatment (Figure 4). A further comparison reveals that ~80%, and ~90% degradation of methyl orange and Congo red within 120-150min of irradiation respectively. The increase of the pH value after visible light irradiation is due to the reduction of surface acidic groups in the ferrite powders, which were introduced during the preparation [33].
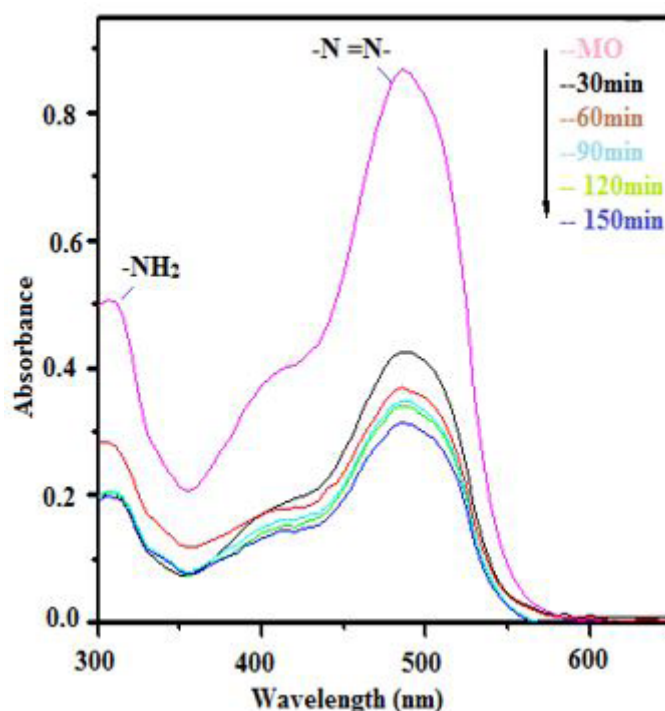
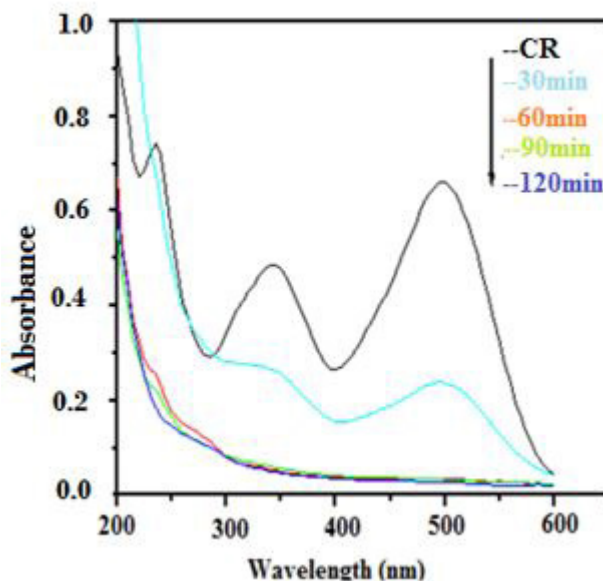**Figure 3:** Effect of irradiation time on Methyl Orange dye

Figure 4: Effect of irradiation time on Congo red dye

Effect Of Catalyst Dose On The Photodecolorization Rate Of Methyl Orange And Congo Red Dyes

As seen in (Figure 5 a&b) and Figure 6 a&b) the increased the doses of catalyst from range (0.5-2.5)g in aqueous solution of methyl orange and Congo red dyes solution were raised the decolonization speed. This behavior indicates to find the many active sites of catalyst surface with increasing the dose. The transmitted light in dye solution is easy transmitted, hence, that entirely leads to enhance the producing of hydroxyl radical. This case will accelerate the decolorization of the dye according to the first possible of Langmuir-Hinshelwood (L-H) kinetics model [34]. The maximum rate constant and PDE % are found at 2.0 g/ 100 mL of $Mg_{0.5}Co_{0.5}Fe_2O_4$ and 85.16% at 70 min and 95.40% at 60 min.

From the other hand, after using 2.5 mg/100 mL of catalyst powder, the rate of reaction depresses, that based on the raised of the solution turbidity and declined the transmittance of light, which caused inhibited the hydroxyl radical formation, this effect is called screen effect. [35-37]
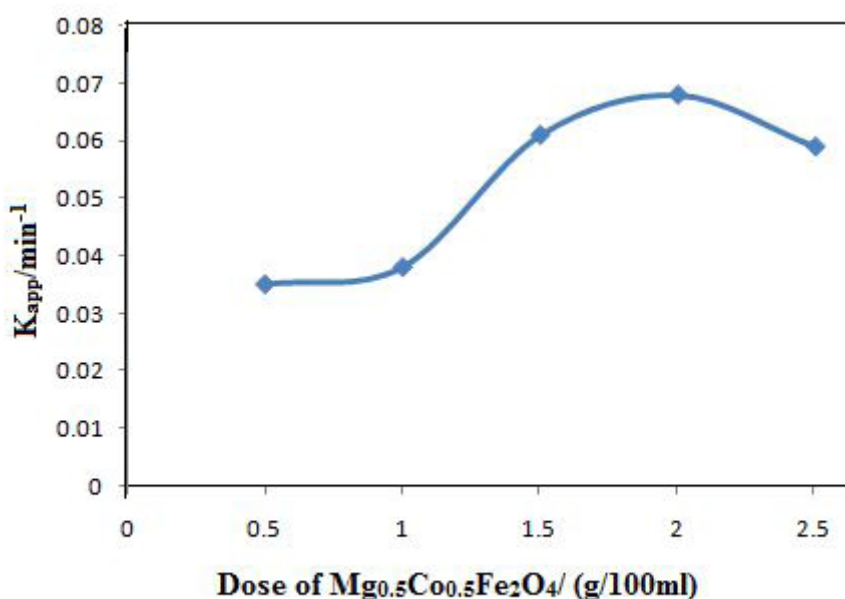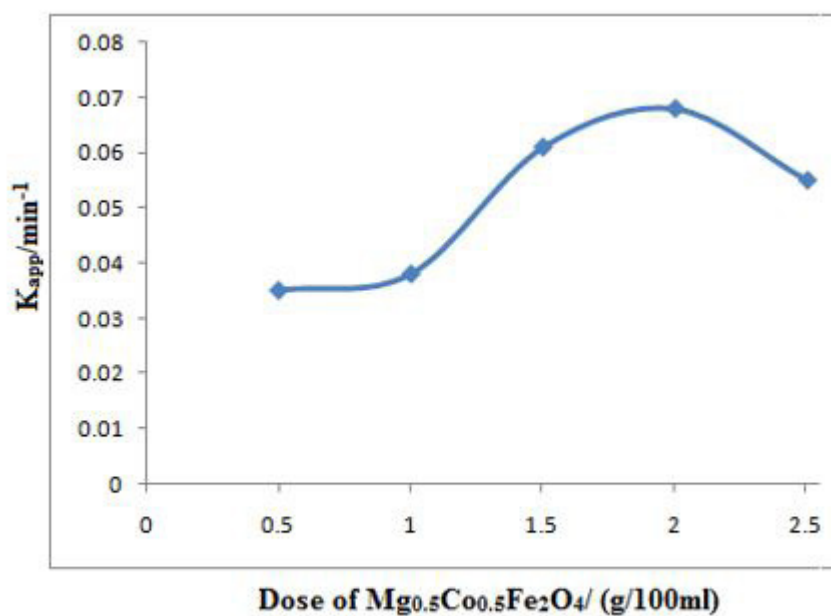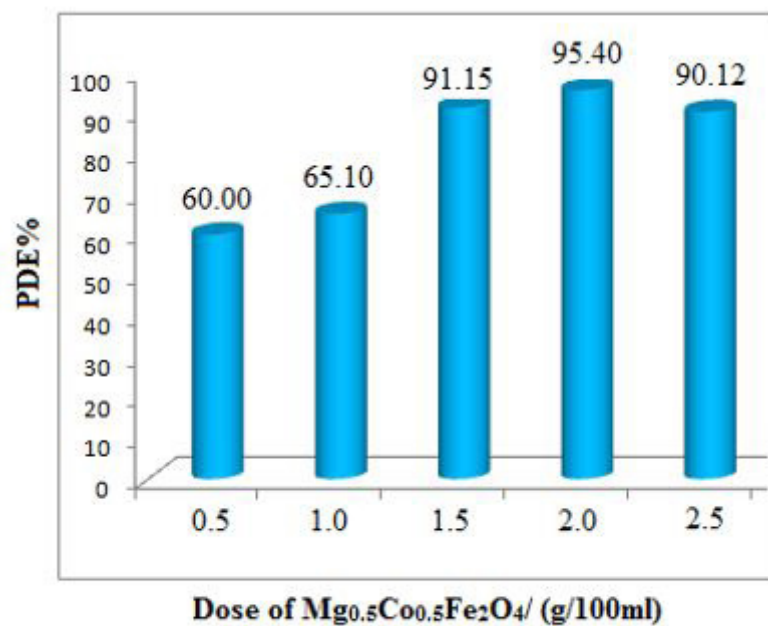

(a)
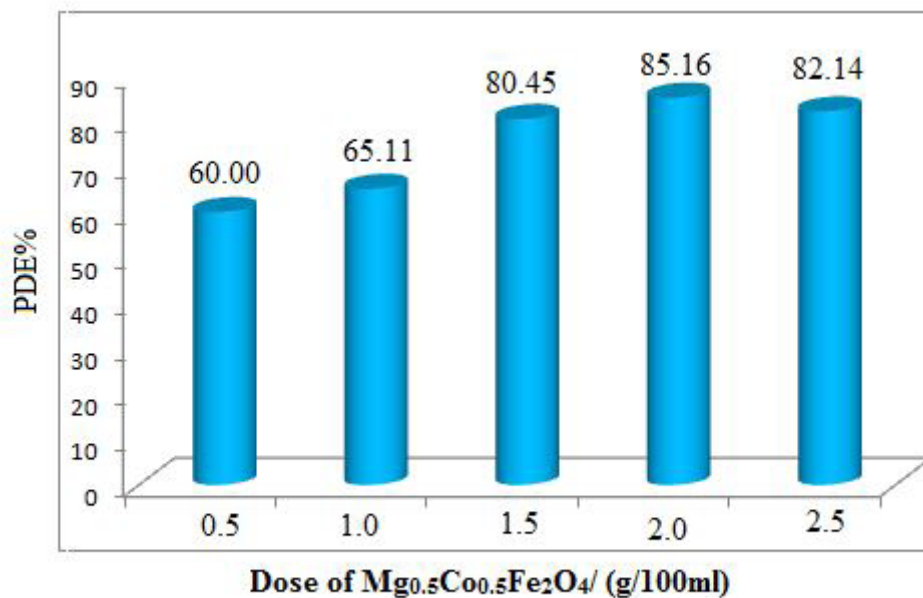
(b)

Figure. 5: Effect of catalyst dose on the (a) apparent rate constant of reaction (b) PDE %, at conditions: cat. dose = (0.5-2.5) g/100mL, methyl orange dye conc.= 30 ppm, initial pH of solution= 5.5 and T= 303K


(a)

(b)

Figure 6: Effect of catalyst dose on the (a) apparent rate constant of reaction (b) PDE %, at conditions: cat. Dose = (0.5-2.5) g/100mL, Congo red dye conc.= 30 ppm, initial pH of solution= 5.5 and T= 303K

Reusability Study of Catalyst

The effect of catalyst after number of runs on the dye solution at conditions: dose (2.0) g/100mL, conc. = 30 ppm, initial pH of solution = 5.5 and T= 303K. The PDE% for Methyl orange is 85.16% and PDE% of Congo red 95.40%. Photodegradation rate further goes on decreases after each successive run (Figure 7 and 8).
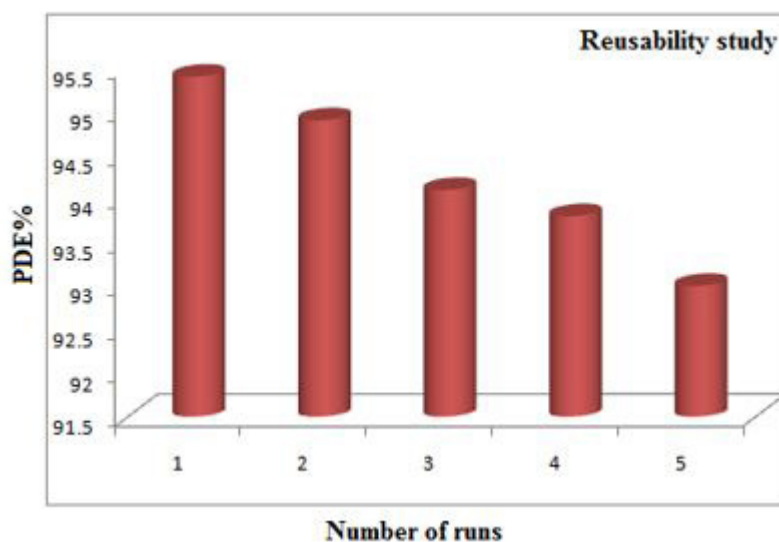
Figure 7: Effect reuse of catalyst at conditions: dose (2.0) g/100mL, conc.= 30 ppm, initial pH of solution= 5.5 and T= 303K for Methyl orange dye
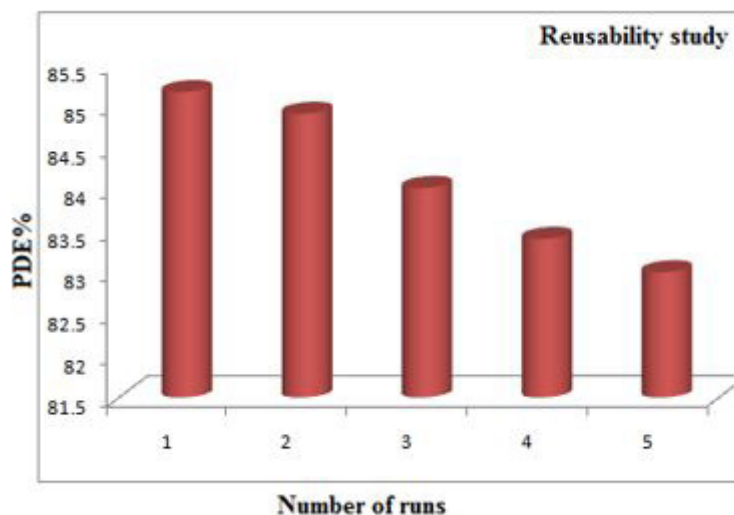
Figure 8: Effect reuse of catalyst at conditions: dose (2.0) g/100mL, conc. = 30 ppm, initial pH of solution= 5.5 and T= 303K for Congo red dye

Mechanisum

In order to form hydroxyl radical on $Mg_{0.5}Co_{0.5}Fe_2O_4$ nanopowder surface must focus a light on the suspension solution. On the basis of the photodecolorization processes described in reference, various redox process can Conducted on surface of photosemiconductor under illumination of UV- A light. Firstly, electron-hole pair (exciton) on catalyst surface was generated. The electron-hole pair is separated by reacting with the other species (H_2O, O_2) in series steps then formed groups of radical intermediates like: superoxide ion O_2^- hydrogen peroxide radical (hydroperoxyl radical) then leads hydroxyl radical Which has a more activity thenHO_2 [38-39].
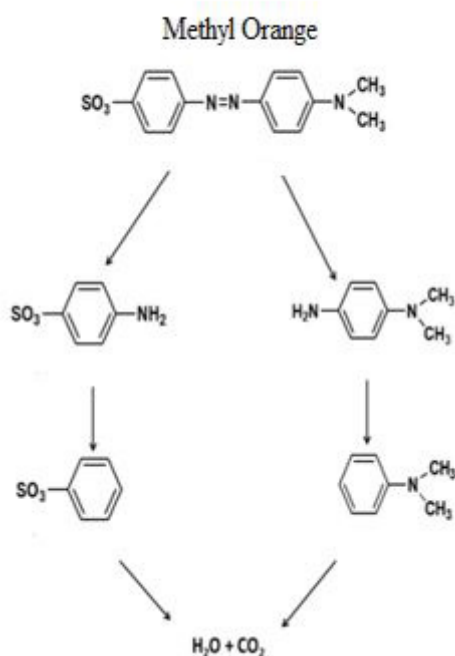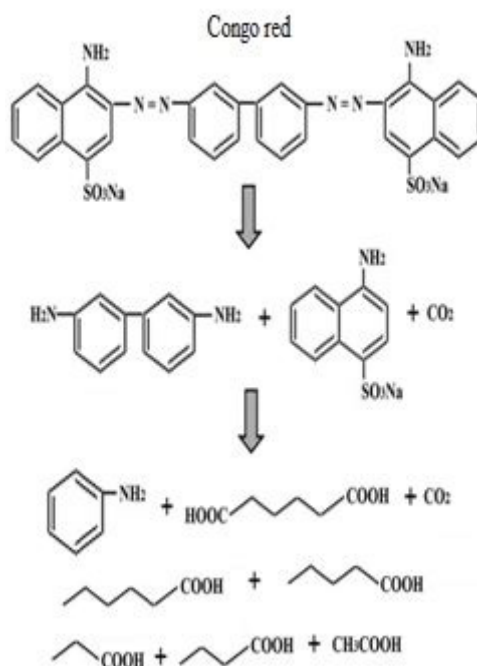
Conclusion

In this study, the main conclusions were observed that the photocatalytic decolorization process of methyl orange and Congo red dyes in suspension solution of $Mg_{0.5}Co_{0.5}Fe_2O_4$ nanopowder under visible light system were carried out. This photoreaction is found to be endothermic and obeyed the pseudo first order with low activation energy. In case of methyl orange the rate of reaction is moderate and same for Congo red it is fast. The PDE% for Methyl orange is 85.16% Ã than PDE% of Congo red 95.40%. Further reuse of catalyst the rate of photodegradation goes on decreases after each successive run

The suitable mechanism was suggested to obtain the depolarization and degradation of this dye with form CO_2 and H_2O (mineralization process) at final pH equal to 7.4.

Acknowledgement

References

1. Shandilya P, Sambyal S, Amit kumar RS (2021) A review: Material research Foundations. 112: 121-161.

2. Mital GS and Manoj T (2011) Review chinese science bulletin 56: 1639-1657

3. Nguyen LTT (2019) Advanced Nanomaterial for Green Growth 25.

4. Dutta SK, Akhter M, Ahmed J, Amin K, Dhar PK Review Biointerface Research in Applied

5. Jang JS, Hong SJ, Lee JS, Borse PH, Kim HG (2009) J Korean Phys Soc 54: 204.

6. Jung ED, Borse PH, Jang JS, Lee JS, Cho CR, et al, (2008) Nanosci Nanotech, 9: 3568.

7. Kim HG, Borse PH, Jang JS, Jeong ED, Jung OS, et al., (2009). Chem Commun 39: 5889.

8. Boumaza S, Boudjemaa A, Bouguelia A, Bouarab R, Trari M, (2010). Appl Energ 87: 2230.

9. Cheng C and Liu CS, (2009). Journal of Physics: Conference Series145: 012028.

10. M. Yokoyama, T. Sato, E. Ohta, and T. Sato (1996) J Appl Phys 80: 1015.

11. Gadkaria A, Shindeb T and Vasambekarc P (2010) Rare metals 29: 168.

12. Silva O, Lima ECD and Morais PC (2003) Journal of Applied Physics 93: 8456

13. Cai C (2016) Appl Catal 182 456-468.

14. Sharma, Bansal S, Singhal S (2015) RSC Adv 5: 6006-6018

15. Dhiman M, Goyal A, Kumar V, Shighal S (2016) New Journal chem 40: 10418-10431.

16. Jadhav SD, Hankare PP, Patil RP and Sasikala R (2011) Materials letters 65: 371-373.

17. Muñoz PG, Fresno F, Víctor de la Peña O'shea, Keller N (2020) Topics in current chemistry, Springer 378.

18. Harish KN, Naik HSB, Prashanth Kumar PN, Vishwanath R and Yashvanth Kumar GS (2013) Archives of Applied Science Research 5: 42-51.

19 .Hankare PP, Patil RP, Pandav RS, Jadhav AV and Jadhav SD (2016) Materials focus 5: 11-16.

20. Mamba G, Mishra AK (2016) Catalysis 6: 79.

21. Ombaka L, Dillert R, Robben L, Bahnemann D (2020) APL Materials 8: 31105

22. Ismael M (2021) Solar energy materials and solar cells 219: 110786

23. Bhekie KKK, Mamba B (2020) Sustainable materials and Technologies 23.

24. Kubacka A, Fern_andez-García M, and Col_G (2012) American Chemical Society Chem 112: 1555-1614.

25. Research & Reviews (2016) Journal of Material Sciences 4.

26. Hankare PP, Kadam MR, Kamble PD, K. Rane KS, Vasambekar PN (2007) Mater Lett 61: 2769.

27. Abbas N, Rubab N, Sadiq N, Manzoor S, Khan MI, et al, (2020) Article Water 12: 1-21

28. Ahmed S (2004) Journal of Photochemistry and Photobiology A: Chemistry 161: 151-154.

29. Sadiqa M, M. Alia M, Amana R, Rashid HUR and Umara MN (2015) Quim Nova 38: 891-895.

30. Mahammed BA, Ahmed LM, (2017) J of Geoscience and Environment Protection 5: 101-111.

31. Liu C, Ronhinone AJ, Zhang Z, (2000) Pure Appl Phys

88: 3608.

32. Fang –chang Tasi, Ning Ma,Tai-chin Ching,Yue Xia,-Fu-sheng chuang (2014) Journal of water process engineering, vol. 1: 2-7.

33. Lu Xiaomeng, Xie Jimin, Song Yuanzhi (2007) J mater Sci 42: 6824-6827.

34. Ahmed LM (2018) Asian J Chem 30: 2134.

35. Ahmed LM and Hussein FH (2012) J of Babylon Uni./Pure and Applied Sciences 1: 464.

36. Zuafuani SI and Ahmed LM (2015) Int J Chem Sci 13: 187.

37. Mahammed BA and. Ahmed LM (2017) J of Geoscience and Environment Protection 5: 101.

38. Radović MD, Mitrović JZ, Kostić MM, Bojić DV, Petrović MM, et al., (2015). Hem Ind 69: 657-665.

39. Ahmed LM and Hussein FH (2014) 1st ed, LAP Lambert Academia Published, Germany.